

## Quantum theory of Manakov solitons

Darren Rand,<sup>1,\*</sup> Ken Steiglitz,<sup>2</sup> and Paul R. Prucnal<sup>1</sup>

<sup>1</sup>*Department of Electrical Engineering, Princeton University, Princeton, NJ 08544, USA*

<sup>2</sup>*Department of Computer Science, Princeton University, Princeton, NJ 08544, USA*

(Received 4 February 2005; published 11 May 2005)

A fully quantum mechanical model of two-component Manakov solitons is developed in both the Heisenberg and Schrödinger representations, followed by an analytical, linearized quantum theory of Manakov solitons in the Heisenberg picture. This theory is used to analyze the vacuum-induced fluctuations of Manakov soliton propagation and collision. The vacuum fluctuations induce phase diffusion and dispersion in Manakov soliton propagation. Calculations of the position, polarization angle, and polarization state fluctuations show an increase in collision-induced noise with a decrease in the relative velocity between the two solitons, as expected because of an increase in the interaction length. Fluctuations in both the polarization angle and state are shown to be independent of propagation distance, opening up possibilities for communications, switching, and logic, exploiting these properties of Manakov solitons. Calculations of the phase noise reveal, surprisingly, that the collision-induced fluctuations can be reduced slightly below the level of fluctuations in the absence of collision, due to cross-correlation effects between the collision-induced phase and amplitude fluctuations of the soliton. The squeezing effect of Manakov solitons is also studied and proven, unexpectedly, to have the same theoretical optimum as scalar solitons.

DOI: 10.1103/PhysRevA.71.053805

PACS number(s): 42.50.Ct, 42.50.Lc, 42.65.Tg, 42.81.Dp

### I. INTRODUCTION

In classical field theory, solitons propagate undistorted in the absence of perturbations. Quantum mechanically, however, solitons undergo phase diffusion and wave packet spreading during propagation [1–4]. Experimental evidence has confirmed these effects [5,6], which have been the topic of recent reviews [7,8].

In this paper, we investigate the quantum theory of Manakov soliton propagation and collision. Manakov solitons are a specific integrable instance of two-component vector solitons described by a coupled set of Schrödinger equations with cubic nonlinearity, solved by the method of inverse scattering in 1973 [9]. Recently, it has been shown that Manakov solitons demonstrate much more complex collision behavior than scalar, one-component solitons. By deriving a general two-soliton solution for the Manakov system, Radhakrishnan *et al.* [10] showed that collisions are characterized not only by a phase and position shift (similar to scalar soliton collisions), but also an intensity redistribution between the two component fields. This last property makes possible different applications for Manakov solitons, including collision-based logic and universal computation [11–14]. Experimentally, energy-exchanging collisions [15] and information transfer [16] have been demonstrated in photorefractive crystals. There exist several candidates for the physical realization of Manakov solitons, including photorefractive crystals [15–19], semiconductor waveguides [20], quadratic media [21], optical fiber [22], and Bose-Einstein condensates [23].

Several approaches have been developed to study the quantum theory of pulse propagation in nonlinear media.

Carter *et al.* [1] and Drummond and Carter [2] numerically solved the scalar quantum nonlinear Schrödinger equation (QNLSE) based on a linearization approximation. The use of the positive-P representation transformed the QNLSE into stochastic nonlinear equations with noise terms. Later, this approach was extended to a vector, two-component theory [24] to study the squeezing spectrum of orthogonal polarizations of light in a birefringent medium [25]. The theory of scalar solitons was studied also in the Schrödinger picture using the Bethe's ansatz method to construct bound-state eigensolutions [26], as well as an approximate analysis based on the Hartree approximation [3]. Another approach uses the Wigner representation to derive approximate stochastic equations [27]. Finally, a linearized approach to quantum solitons, developed by Haus and Lai [4], takes the classical soliton as the expectation value of the quantized field. Quantum effects appear as a perturbation to the classical field, upon which are projected statistics correlated to a zero-point fluctuation background, or vacuum fluctuations. This method forms the basis for the analytical results of this study, which has also been applied to second-order [28] and self-induced transparency solitons [29].

This paper is organized as follows. In Sec. II, we quantize the two-component field and derive the coupled QNLSE in both the Schrödinger and Heisenberg representations. Section III reviews Manakov soliton perturbation theory, in which the soliton is parametrized into six operators. In Sec. IV, we calculate uncertainties in these soliton operators and fully characterize the vacuum-induced fluctuations of these operators during propagation and collision. These computations reveal that the variance of fluctuations for soliton position, polarization angle, and polarization state increase as the relative velocity between colliding solitons decreases, as expected, because of an increase in the interaction length. But, different effects in the variance of the phase fluctuations arise, showing that the level of fluctuations after a collision

\*Electronic address: drand@princeton.edu

can fall slightly below the variance level in the absence of collision. All these fluctuations can provide both a limit on the performance of communication or computation systems that rely on propagation and interaction of Manakov solitons, as well as guide future experiments confirming such effects. In Sec. V, we show, surprisingly, that optimal detection of squeezing in Manakov and scalar solitons is equivalent.

## II. COUPLED QUANTUM NONLINEAR SCHRÖDINGER EQUATION

The Hamiltonian describing a dispersive, two-component system with nonlinear interaction is given by [30,31]

$$\hat{H} = -\hbar \int dx \left( \sum_{\lambda=1}^2 \frac{\partial}{\partial x} \hat{u}_{\lambda}^{\dagger} \frac{\partial}{\partial x} \hat{u}_{\lambda} + \mu (\hat{u}_1^{\dagger} \hat{u}_1^{\dagger} \hat{u}_1 \hat{u}_1 + \hat{u}_2^{\dagger} \hat{u}_2^{\dagger} \hat{u}_2 \hat{u}_2 + 2\hat{u}_1^{\dagger} \hat{u}_2^{\dagger} \hat{u}_2 \hat{u}_1) \right), \quad (1)$$

where normal ordering of the field operators has been adopted. The quantum field amplitude operators  $\hat{u}_{\lambda}$  and  $\hat{u}_{\lambda}^{\dagger}$  correspond to annihilation and creation operators, respectively, where  $\lambda=1,2$  represents the field component. The normalized time deviation from the pulse center  $x$  travels in a reference frame at the average group velocity of the two field components  $\hat{u}_1$  and  $\hat{u}_2$ , and the normalized parameter  $\mu$  represents the magnitude of the cubic (Kerr) nonlinearity. We assume a lossless medium with an instantaneous electronic response, which is valid for picosecond pulses propagating in optical fiber for distances on the order of 1 km. The dimensionless photon density in these scaled units is  $\bar{\mu} |\hat{u}_{\lambda}^{\dagger} \hat{u}_{\lambda}|$ , where  $\bar{\mu}$  is a characteristic photon number scale that depends on the given physical system. The first term in Eq. (1) represents second-order dispersion, with higher-order dispersion neglected, while the remaining terms are interaction terms, which here describe self- and cross-phase modulation due to the Kerr nonlinearity.

The field operators  $\hat{u}_{\lambda}(x)$  and  $\hat{u}_{\lambda}^{\dagger}(x)$  are normalized in such a way that they obey the bosonic equal-space commutation relations

$$[\hat{u}_{\lambda}(x'), \hat{u}_{\lambda'}^{\dagger}(x)] = \delta_{\lambda\lambda'} \delta(x-x'), \quad (2)$$

where  $\lambda, \lambda'=1,2$  and all other operators commute. Here we choose equal-space commutation relations as opposed to the more formal equal-time commutation relations. Agreement between these two approaches has been shown previously [32].

The system described by the Hamiltonian of Eq. (1) can be analyzed using both the Schrödinger and Heisenberg representations. In the Heisenberg picture, in which  $(\partial/\partial z)\hat{u}_{\lambda}(x,z) = -(i/\hbar)[\hat{u}_{\lambda}(x,z), \hat{H}]$ , where  $z$  is the normalized propagation distance, we can derive the coupled QNLSE

$$i \frac{\partial \hat{u}_1}{\partial z} + \frac{\partial^2 \hat{u}_1}{\partial x^2} + 2\mu(\hat{u}_1^{\dagger} \hat{u}_1 + \hat{u}_2^{\dagger} \hat{u}_2) \hat{u}_1 = 0,$$

$$i \frac{\partial \hat{u}_2}{\partial z} + \frac{\partial^2 \hat{u}_2}{\partial x^2} + 2\mu(\hat{u}_1^{\dagger} \hat{u}_1 + \hat{u}_2^{\dagger} \hat{u}_2) \hat{u}_2 = 0. \quad (3)$$

Alternatively, in the Schrödinger picture, we define a state vector,  $|\psi(z)\rangle$ , which is time dependent, and the quantum operators are those at  $z=0$ . The Schrödinger equation for the state vector is

$$i\hbar \frac{d}{dz} |\psi(z)\rangle = \hat{H} |\psi(z)\rangle, \quad (4)$$

where the state  $|\psi(z)\rangle$  can be expanded in Fock space as

$$|\psi(z)\rangle = \sum_l a_l \int dx_1, \dots, dx_n dx_{n+1}, \dots, dx_{n+m} \times f_{nm}(x_1, \dots, x_n, x_{n+1}, \dots, x_{n+m}, z) \times \prod_{i=1}^n \hat{u}_1^{\dagger}(x_i) \prod_{j=1}^m \hat{u}_2^{\dagger}(x_{n+j}) |0\rangle. \quad (5)$$

In this expansion,  $|0\rangle$  is the two-component vacuum,  $f_{nm}$  is a normalized wave function for the  $n+m$  particle system— $n$  particles in mode 1,  $m$  particles in mode 2. The complex coefficients  $a_l$  determine the photon statistics of the pulse.

Although exact eigenfunctions of  $\hat{H}$  can be constructed, it becomes technically inconvenient for a large number of bosons. In such cases, we can use the Hartree approximation [33], which, essentially, determines the behavior of each boson in the presence of all the others. Each boson then feels the same mean-field potential, and the many-body wave function  $f_{nm}$  can be approximated as a product of single-boson wave functions

$$f_{nm} = \prod_{i=1}^n \Phi_n^{(1)}(x_i, t) \prod_{j=1}^m \Phi_{n+m}^{(2)}(x_{n+j}, t), \quad (6)$$

which is normalized by

$$\int |\Phi_{n,n+m}^{(1,2)}|^2 dx = 1. \quad (7)$$

Coupled equations of motion can be obtained for  $\Phi_{n,n+m}^{(1,2)}$  by using the time-dependent Hartree variational method [33], which yields

$$i \frac{\partial \Phi_n^{(1)}}{\partial z} + \frac{\partial^2 \Phi_n^{(1)}}{\partial x^2} + 2\mu[(n-1)|\Phi_n^{(1)}|^2 + m|\Phi_{n+m}^{(2)}|^2] \Phi_n^{(1)} = 0, \\ i \frac{\partial \Phi_{n+m}^{(2)}}{\partial z} + \frac{\partial^2 \Phi_{n+m}^{(2)}}{\partial x^2} + 2\mu[n|\Phi_n^{(1)}|^2 + (m-1)|\Phi_{n+m}^{(2)}|^2] \Phi_{n+m}^{(2)} = 0. \quad (8)$$

As a result of the Hartree approximation, the first of Eqs. (8) shows that the  $n$ th boson of mode 1 interacts, in an identical manner, with both the remaining  $n-1$  bosons of mode 1 and all  $m$  bosons of mode 2, and similarly for the second equation. Equations (8) exactly coincide with the classical Manakov equations [9] in the high photon number limit, in which  $n \sim m \gg 1$ . We have thus formulated the problem in both the Schrödinger and Heisenberg pictures. In this paper, we will

investigate the quantum properties of Manakov solitons at high photon number in the Heisenberg picture, since it lends itself to a more straightforward analysis using classical perturbation theory techniques.

The coupled QNLSE, Eq. (3), can be written in vector form as

$$i\frac{\partial}{\partial z}\hat{\Psi} + \frac{\partial^2}{\partial x^2}\hat{\Psi} + 2\mu(\hat{\Psi}^\dagger\hat{\Psi})\hat{\Psi} = 0, \quad (9)$$

where  $\hat{\Psi} \equiv \begin{bmatrix} \hat{u}_1 \\ \hat{u}_2 \end{bmatrix}$  and  $\hat{\Psi}^\dagger$  is the transposed complex conjugate of  $\hat{\Psi}$ . The form of the classical fundamental Manakov soliton solution is [9]

$$\begin{aligned} \Psi_0 &\equiv \begin{bmatrix} u_{10} \\ u_{20} \end{bmatrix} \\ &= \frac{A_0}{2} \begin{bmatrix} \cos(\phi)\exp(i\theta_1) \\ \sin(\phi)\exp(i\theta_2) \end{bmatrix} \exp\left[i\left(k_x x + \frac{A_0^2}{4}z - k_x^2 z\right)\right] \\ &\quad \times \operatorname{sech}\left[\frac{A_0}{2}(x - x_0 - 2k_x z)\right], \end{aligned} \quad (10)$$

where we set  $\mu=1$ , corresponding to the case of anomalous dispersion where Eq. (9) admits bright soliton solutions. This solution has six arbitrary integration constants (as opposed to four in scalar soliton theory). They have been chosen so that  $A_0$  is the scaled amplitude, defined in such a way that  $\int(|u_{10}|^2 + |u_{20}|^2)dx = A_0$ ,  $x_0$  is the initial position,  $k_x$  is the momentum per photon (frequency),  $\theta_{1,2}$  is the phase of each component, and  $\phi$  represents the ratio between the absolute amplitudes of the vector components. For a Manakov soliton composed of two orthogonal polarizations,  $\phi$  is the polarization angle.

### III. QUANTUM PERTURBATION THEORY FOR MANAKOV SOLITONS

Following the formalism of Haus and Lai [4], we introduce the following perturbation into Eq. (9):

$$\hat{\Psi} = \Psi_0 + \Delta\hat{\Psi}, \quad (11)$$

where  $\Delta\hat{\Psi} \equiv \begin{bmatrix} \Delta\hat{u}_1 \\ \Delta\hat{u}_2 \end{bmatrix}$ , subject to the commutation relation

$$[\Delta\hat{u}_\lambda(x', z), \Delta\hat{u}_\lambda^\dagger(x, z)] = \delta_{\lambda\lambda'}\delta(x - x'). \quad (12)$$

This linearization separates the field operator  $\hat{\Psi}$  into its mean value  $\Psi_0$ , the solution to the classical Manakov equations, and a remainder  $\Delta\hat{\Psi}$ , which describes the quantum fluctuations and takes over the commutation relation of  $\hat{\Psi}$ , as shown in Eq. (12). Classical vector soliton interactions based on this linearization approximation were investigated recently [34]. Our treatment uses similar perturbation theory techniques, but with a quantum mechanical perturbation term that describes vacuum fluctuations. The validity of this approach in soliton theory has been confirmed; corrections to the linearization were calculated using the Bethe ansatz solutions, where it was shown that, for high photon number  $\bar{\mu}$  and phase shifts up to  $\bar{\mu}^{1/4}$ , the use of the classical solution as

the mean field and the quantum noise as the perturbation is justified [3,35]. For typical photon numbers of  $10^9$ , this approximation is valid for propagation lengths on the order of 1 km in optical fiber.

Substituting Eq. (11) into the coupled QNLSE and linearizing in terms of  $\Delta\hat{u}_1$ ,  $\Delta\hat{u}_2$  gives the following coupled set of equations:

$$\begin{aligned} i\frac{\partial\Delta\hat{u}_1}{\partial z} + \frac{\partial^2\Delta\hat{u}_1}{\partial x^2} + 2[(2|u_{10}|^2 + |u_{20}|^2)\Delta\hat{u}_1 + u_{10}^2\Delta\hat{u}_1^\dagger \\ + u_{20}^*u_{10}\Delta\hat{u}_2 + u_{20}u_{10}\Delta\hat{u}_2^\dagger] = 0, \end{aligned} \quad (13)$$

where the accompanying equation for  $\Delta\hat{u}_2$  can be found by interchanging the subscripts 1 and 2. In general,  $\Delta\hat{\Psi}$  can be expanded as  $\Delta\hat{\Psi} = \Delta\hat{\Psi}_{\text{sol}} + \Delta\hat{\Psi}_{\text{cont}}$ . In this expansion, the perturbation has been separated into two parts: a part  $\Delta\hat{\Psi}_{\text{sol}}$ , which describes changes in the soliton parameters, and a part  $\Delta\hat{\Psi}_{\text{cont}}$  due to dispersive waves that radiate from the perturbed soliton field, called the continuum. The first term  $\Delta\hat{\Psi}_{\text{sol}}$  can be expanded to describe the changes in the six soliton parameters. Since derivatives of the classical fundamental Manakov soliton solution [Eq. (10)] with respect to the soliton parameters  $A_0$ ,  $x_0$ ,  $k_x$ ,  $\theta_{1,2}$ , and  $\phi$  are solutions to Eq. (13), the expansion is

$$\begin{aligned} \Delta\hat{\Psi}_{\text{sol}} &= \sum_m f_m(x, z)\Delta\hat{m}(z)\exp(i\Phi(z)), \\ m &\in \{A_0, x_0, k_x, \theta_1, \theta_2, \phi\}, \end{aligned} \quad (14)$$

where basis vectors  $f_m(x, z) \equiv (\partial\Psi_0/\partial m)|_{x_0=k_x=0}$ , classical phase shift  $\Phi(z) \equiv (A_0^2/4)z$ , and  $\Delta\hat{m}(z)$  represents the quantum fluctuations of each soliton parameter. Without loss of generality, we have selected a reference frame moving with the soliton in such a way that  $x_0 = k_x = 0$ . The vectors  $f_m$  obey a biorthonormal relationship with adjoint vectors  $g_m$ , satisfying

$$\begin{aligned} \operatorname{Re}\left(\int g_m^\dagger f_n dx\right) &= \delta_{mn}, \quad m, n \in \{A_0, x_0, k_x, \theta_1, \theta_2, \phi\}. \\ & \quad (15) \end{aligned}$$

The vectors  $f_m$  and  $g_m$  are given in the Appendix.

As in the case of scalar solitons, the six basis functions  $f_m(x, z)$  can be written explicitly as linear combinations of the six basis functions  $f_m(x, z)|_{z=0}$  and  $z$ . Given this property, it was shown that excitations of the continuum are orthogonal to excitations of the soliton parameters [29]. In addition, the continuum disperses out totally at  $z \rightarrow \infty$ . For these reasons, we can neglect the continuum in the analysis that follows. It should be noted that a full set of excitation modes, including the continuum, has been found for the case of scalar and Manakov solitons in Refs. [36,37], respectively.

### IV. FLUCTUATION OPERATORS

The quantum fluctuations of the six parameters can be obtained by inverting the expansion in Eq. (14) to give

$$\Delta\hat{m}(z) = \text{Re} \left\{ \int g_m^\dagger(x) \exp[-i\Phi(z)] \Delta\hat{\Psi}(x, z) dx \right\}, \quad (16)$$

where multiplication by the phase factor  $\exp(-i\Phi(z))$  cancels the mean phase shift. Using Eq. (16), the following pairs of noncommuting operators can be calculated:

$$\begin{aligned} [\Delta\hat{A}_0, \Delta\hat{\theta}_1] &= [\Delta\hat{A}_0, \Delta\hat{\theta}_2] = i, \\ [A_0\Delta\hat{\phi}, \Delta\hat{\theta}_1] &= -\frac{i}{2} \tan(\phi), \\ [A_0\Delta\hat{\phi}, \Delta\hat{\theta}_2] &= \frac{i}{2} \cot(\phi), \\ [\Delta\hat{x}_0, A_0\Delta\hat{k}_x] &= i, \end{aligned} \quad (17)$$

where all other pairs of operators commute. The first three relations are photon number and phase commutators, whereas the last is the commutation relation for momentum and position. Since these commutators are conserved during evolution, we have quantized the soliton excitation successfully and there is no need to introduce additional noise sources. A word of caution is in order. At values of  $\phi$  approaching 0 or  $\pi/2$ , singularities in these commutators appear. At these values, a majority of photons are in one component of the soliton, where the scaled amplitudes of each component are proportional to  $A_0 \cos \phi$  and  $A_0 \sin \phi$ . However, our linearization assumes a large photon number. Therefore, these amplitude and phase relations do not hold in this approximation for all values of  $\phi$ . As a result, the theory developed here is limited to Manakov solitons in which both components have a substantially high photon number [35]. To establish a conservative estimate on the allowable range of  $\phi$ , we will assume pulses with photon numbers of  $10^9$  to propagate 100 m, an order of magnitude greater than the distance for which quantum effects become experimentally observable [5]. Using these parameters, values of  $1^\circ < \phi < 89^\circ$  will be valid for the chosen linearization. For other values of  $\phi$ , we demonstrate later in this section that the soliton fluctuations approach the scalar soliton fluctuations because of a correspondence that arises at these limits.

### A. Propagation

In order to calculate the initial variances of the fluctuation operators, we assume that the soliton is initially in a uniform zero-point fluctuation background, so that  $\langle \Delta\hat{u}_\lambda \Delta\hat{u}_\lambda^\dagger \rangle = \delta_{\lambda\lambda'} \delta(x-x')$ ,  $\lambda=1, 2$ , and all other correlations vanish. This state is chosen because it contains a minimal amount of initial quantum noise and represents accurately the radiation from a mode-locked laser. We can therefore compute the variances of the vacuum-induced fluctuations using Eq. (16) at  $z=0$

$$\langle \Delta\hat{A}_0^2 \rangle_0 = \frac{1}{4} \int (|g_{1A}(x)|^2 + |g_{2A}(x)|^2) dx = A_0,$$

$$\langle \Delta\hat{x}_0^2 \rangle_0 = \frac{1}{4} \int (|g_{1x}(x)|^2 + |g_{2x}(x)|^2) dx = \frac{\pi^2}{3A_0^3},$$

$$\langle \Delta\hat{k}_x^2 \rangle_0 = \frac{1}{4} \int (|g_{1k}(x)|^2 + |g_{2k}(x)|^2) dx = \frac{A_0}{12},$$

$$\langle \Delta\hat{\phi}^2 \rangle_0 = \frac{1}{4} \int (|g_{1\phi}(x)|^2 + |g_{2\phi}(x)|^2) dx = \frac{1}{4A_0},$$

$$\langle \Delta\hat{\theta}_1^2 \rangle_0 = \frac{1}{4} \int |g_{1\theta}(x)|^2 dx = \frac{1}{3} \left( 1 + \frac{\pi^2}{12} \right) \frac{1}{A_0 \cos^2 \phi},$$

$$\langle \Delta\hat{\theta}_2^2 \rangle_0 = \frac{1}{4} \int |g_{2\theta}(x)|^2 dx = \frac{1}{3} \left( 1 + \frac{\pi^2}{12} \right) \frac{1}{A_0 \sin^2 \phi}. \quad (18)$$

The uncertainty products of the photon number and phase are

$$\begin{aligned} \langle [\Delta(\hat{A}_0 \cos \hat{\phi})]^2 \rangle_0 \langle \Delta\hat{\theta}_1^2 \rangle_0 &= \frac{1}{12} \left( 1 + \frac{\pi^2}{12} \right) \left( 3 + \frac{1}{\cos^2 \phi} \right) \gtrsim 0.61, \\ \langle [\Delta(\hat{A}_0 \sin \hat{\phi})]^2 \rangle_0 \langle \Delta\hat{\theta}_2^2 \rangle_0 &= \frac{1}{12} \left( 1 + \frac{\pi^2}{12} \right) \left( 3 + \frac{1}{\sin^2 \phi} \right) \gtrsim 0.61, \end{aligned} \quad (19)$$

where the photon number uncertainty in each component is given by  $\Delta(\hat{A}_0 \cos \hat{\phi})$  and  $\Delta(\hat{A}_0 \sin \hat{\phi})$ , and the uncertainty product for momentum and position is

$$A_0^2 \langle \Delta\hat{k}_x^2 \rangle_0 \langle \Delta\hat{x}_0^2 \rangle_0 \approx 0.27. \quad (20)$$

Like the scalar soliton, the Manakov soliton combines properties characteristic of both waves and particles and possesses pairs of operators describing both properties. The uncertainty products in Eq. (19) show the photon number and phase relationship characteristic of a wave, and Eq. (20) describes the position and momentum uncertainty product characteristic of a particle. The lower bound on the first two expressions corresponds exactly to the uncertainty product for scalar solitons [4]. These inequalities reach the lower bound at the excluded values of  $\phi=0$  and  $\pi/2$ , representing a correspondence between the Manakov and scalar cases, which should arise at these extremal values.

From Eq. (16), the fluctuation operators  $\Delta\hat{m}(z)$  at any position  $z$  are

$$\Delta\hat{A}_0(z) = \Delta\hat{A}_0(0),$$

$$\Delta\hat{x}_0(z) = \Delta\hat{x}_0(0) + 2\Delta\hat{k}_x(0)z,$$

$$\Delta\hat{k}_x(z) = \Delta\hat{k}_x(0),$$

$$\Delta\hat{\phi}(z) = \Delta\hat{\phi}(0),$$

$$\Delta\hat{\theta}_1(z) = \Delta\hat{\theta}_1(0) + \frac{A_0}{2} \Delta\hat{A}_0(0)z,$$

$$\Delta \hat{\theta}_2(z) = \Delta \hat{\theta}_2(0) + \frac{A_0}{2} \Delta \hat{A}_0(0)z. \quad (21)$$

Consistent with scalar soliton theory, Eqs. (21) show that phase and position become correlated with amplitude and momentum, respectively. As a result, the soliton experiences phase diffusion and wave packet spreading, while the amplitudes of each component and the momentum propagate unchanged. The term responsible for wave packet spreading,  $\Delta \hat{x}_0(z)$ , can be attributed to the group velocity dispersion of the Kerr medium, while the phase diffusion terms,  $\Delta \hat{\theta}_1(z)$  and  $\Delta \hat{\theta}_2(z)$ , result from the combined effects of self- and cross-phase modulation. It should be noted that these propagation-induced fluctuations do not present a fundamental limit to the performance of a particular application. In fact, it was shown that both of these propagation-dependent effects can be canceled with the insertion of a near-resonant two-level system [38,39].

From Eqs. (18) and (21), the variances of the six soliton parameters at some arbitrary point  $z$  are

$$\langle \Delta \hat{A}_0^2(z) \rangle = A_0,$$

$$\langle \Delta \hat{x}_0^2(z) \rangle = \frac{\pi^2}{3A_0^3} + \frac{A_0}{3} z^2,$$

$$\langle \Delta \hat{k}_x^2(z) \rangle = \frac{A_0}{12},$$

$$\langle \Delta \hat{\phi}^2(z) \rangle = \frac{1}{4A_0},$$

$$\langle \Delta \hat{\theta}_1^2(z) \rangle = \frac{1}{3} \left( 1 + \frac{\pi^2}{12} \right) \frac{1}{A_0 \cos^2(\phi)} + \frac{A_0^3}{4} z^2,$$

$$\langle \Delta \hat{\theta}_2^2(z) \rangle = \frac{1}{3} \left( 1 + \frac{\pi^2}{12} \right) \frac{1}{A_0 \sin^2(\phi)} + \frac{A_0^3}{4} z^2. \quad (22)$$

These six equations describe fully the evolution of vacuum noise for the six parameters of a Manakov soliton in the absence of collision. The initial frequency fluctuations cause a quadratic increase in the variance of position fluctuations as a function of propagation distance due to the group velocity dispersion of the medium. In addition, the variance of phase fluctuations of each component increases quadratically with propagation as a result of zero-point amplitude fluctuations, which couple to the Kerr nonlinearity. Amplitude fluctuations obey Poisson statistics, and the variance of polarization angle fluctuations, an identifying characteristic of vector solitons, is independent of the distance propagated.

### B. Collision

It has been shown previously that vacuum noise causes sufficient wave packet spreading to give rise to large error rates in cascaded logic gates based on scalar soliton collisions [40]. Calculating the vacuum-induced fluctuations of

Manakov solitons can be applied similarly, in order to investigate whether quantum noise will present similar obstacles toward the realization of switching, logic, and computation based on Manakov solitons [11–14]. In addition, this theory can be applied in the planning of new experiments to test quantum effects in this coupled system.

A collision between scalar solitons induces a phase shift and a time (or, equivalently, position) shift [41]. Manakov soliton collisions demonstrate these same effects, with an additional collision process that involves an intensity redistribution between the two component fields  $u_{10}$  and  $u_{20}$  [10]. This last property has been applied recently to show collision-based logic and universal computation [11–14].

A quantum description of scalar soliton collisions has been treated by several authors, primarily in the context of quantum nondemolition measurements [30,40,42,43]. In order to study the quantum fluctuations in a collision of two Manakov solitons, we assume that both solitons are initially well separated in space, in such a way that they can be treated as the sum of two independent fundamental solitons. The perturbation of each soliton can then be decomposed into a linear combination of its six fluctuation operators. After collision, however, the solitons become quantum-mechanically entangled. Therefore, the twelve (six for each soliton) post-collision operators will depend nontrivially on the precollision operators. As in our previous analysis, we neglect the noise contributions that arise as a result of interactions between the continuous spectrum and each soliton field.

The classical position shift of soliton 1 after a collision with soliton 2 is given by [44]:

$$\delta x^{(1)} = \frac{A_0^{(1)} + A_0^{(2)}}{A_0^{(1)} A_0^{(2)}} \ln \left( \frac{|k^{(1)} - k^{(2)}|^2}{|k^{(1)} + k^{(2)*}|^2} \left[ 1 - \frac{A_0^{(1)} A_0^{(2)}}{|k^{(1)} + k^{(2)*}|^2} |\alpha_1^{(1)} \alpha_1^{(2)*} + \alpha_2^{(1)} \alpha_2^{(2)*}|^2 \right] \right), \quad (23)$$

where  $k^{(j)} \equiv [A_0^{(j)}/2] + ik_x^{(j)}$ ,  $\alpha_1^{(j)} \equiv \cos \phi^{(j)} \exp(i\theta_1^{(j)})$ ,  $\alpha_2^{(j)} \equiv \sin \phi^{(j)} \exp(i\theta_2^{(j)})$ ,  $j=1,2$  is the soliton number, and  $k_x^{(1)} > k_x^{(2)}$ .

The position fluctuation in soliton 1 because of the collision can be calculated by

$$\Delta \delta \hat{x}^{(1)} = \sum_m \frac{\partial \delta x^{(1)}}{\partial m} \Delta \hat{m}(0),$$

$$m \in \{A_0^{(j)}, k_x^{(j)}, \theta_1^{(j)}, \theta_2^{(j)}, \phi^{(j)}\}. \quad (24)$$

The overall fluctuation of the position operator of soliton 1 can therefore be generalized from Eq. (21) to include one collision

$$\Delta \hat{x}_0^{(1)}(z) = \Delta \hat{x}_0^{(1)}(0) + 2\Delta \hat{k}_x^{(1)}(0)z + \Delta \delta \hat{x}^{(1)}. \quad (25)$$

The variance of soliton position after one collision can likewise be calculated

$$\langle \Delta \hat{x}_0^{(1)2}(z) \rangle = \frac{\pi^2}{3A_0^{(1)3}} + \frac{A_0^{(1)}}{3} z^2 + \frac{A_0^{(1)}}{3} \frac{\partial \delta x^{(1)}}{\partial k_x^{(1)}} z + \langle \Delta \delta \hat{x}^{(1)2} \rangle. \quad (26)$$

The last two terms in Eq. (26) arise due to collision, in which the first results from a cross-correlation between the fluctuations in velocity,  $\Delta \hat{k}_x^{(1)}(0)$ , and the collision-induced position shift.

The classical postcollision polarization and carrier phase of soliton 1,  $\alpha_i^{(1)+}$ , after a collision with soliton 2 are described by [44]

$$\alpha_i^{(1)+} = \frac{\alpha_i^{(1)} - \frac{A_0^{(2)}}{k^{(1)} + k^{(2)*}} (\alpha_1^{(1)} \alpha_1^{(2)*} + \alpha_2^{(1)} \alpha_2^{(2)*}) \alpha_i^{(2)}}{\left[ 1 - \frac{A_0^{(1)} A_0^{(2)}}{|k^{(1)} + k^{(2)*}|^2} |\alpha_1^{(1)} \alpha_1^{(2)*} + \alpha_2^{(1)} \alpha_2^{(2)*}|^2 \right]^{1/2}}, \quad (27)$$

where  $i=1,2$  is the soliton component. The variances  $\langle \Delta \hat{\phi}^2(z) \rangle$ ,  $\langle \Delta \hat{\theta}_1^2(z) \rangle$ , and  $\langle \Delta \hat{\theta}_2^2(z) \rangle$  can be determined from Eq. (27) to include collisions in the same manner as  $\langle \Delta \hat{x}_0^{(1)2}(z) \rangle$ . By straightforward manipulation of Eq. (27), an expression can be obtained for the collisional phase and polarization angle shifts  $\delta \theta_i^{(1)}$  and  $\delta \phi^{(1)}$ . The total variance of soliton phase and polarization angle after one collision is then given by

$$\langle \Delta \hat{\theta}_i^{(1)2}(z) \rangle = \langle \Delta \hat{\theta}_i^{(1)2}(0) \rangle + \frac{A_0^{(1)3}}{4} z^2 + A_0^{(1)2} \frac{\partial \delta \theta_i^{(1)}}{\partial A_0^{(1)}} z + 2 \frac{\partial \delta \theta_i^{(1)}}{\partial \theta_i^{(1)}} \langle \Delta \hat{\theta}_i^{(1)2}(0) \rangle + \langle \Delta \delta \hat{\theta}_i^{(1)2} \rangle, \quad (28a)$$

$$\langle \Delta \hat{\phi}^{(1)2}(z) \rangle = \frac{1}{4A_0} + \frac{1}{2A_0} \frac{\partial \delta \phi^{(1)}}{\partial \phi^{(1)}} + \langle \Delta \delta \hat{\phi}^{(1)2} \rangle, \quad (28b)$$

where  $\Delta \delta \hat{\theta}_i^{(1)}$  and  $\Delta \delta \hat{\phi}^{(1)}$  are defined in the same way as  $\Delta \delta \hat{x}^{(1)}$  in Eq. (24). It is remarkable that the variance of polarization angle is independent of propagation distance.

Due to the quadratic dependencies of  $\langle \Delta \hat{x}_0^{(1)2}(z) \rangle$  and  $\langle \Delta \hat{\theta}_i^2(z) \rangle$  on the scaled propagation distance  $z$ , phase diffusion and wave packet spreading can become limiting factors in communications or computation systems using Manakov solitons, even without considering collisions. As an example,  $\langle \Delta \hat{x}_0^{(1)2}(z) \rangle$ ,  $\langle \Delta \hat{\phi}^2(z) \rangle$ , and  $\langle \Delta \hat{\theta}_1^2(z) \rangle$  are calculated for a two-soliton collision using Eqs. (26) and (28) and plotted in Figs. 1–3, respectively, as both a function of the propagation distance  $z$  and the relative velocity between the colliding solitons. The parameters of soliton 1, 2 for these and all subsequent calculations are:  $A_0=1, 1$ ;  $k_x=0, -\delta k_x$ ;  $\phi=3\pi/10, \pi/6$ ;  $\theta_1=0, 0$ ;  $\theta_2=\pi/3, 2\pi/5$ , unless otherwise noted. The velocity dependence of these effects are investigated by varying the relative velocity  $\delta k_x \equiv k_x^{(1)} - k_x^{(2)}$ . We will concentrate only on one phase operator, noting that the behavior of both  $\langle \Delta \hat{\theta}_1^2(z) \rangle$  and  $\langle \Delta \hat{\theta}_2^2(z) \rangle$  is qualitatively identical for the studied cases.

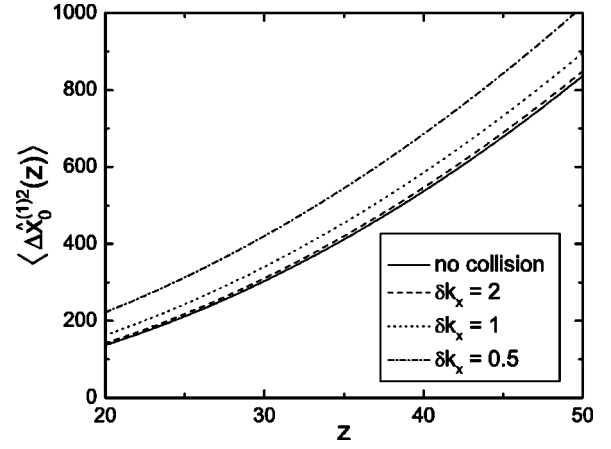


FIG. 1. Variance of position fluctuations  $\langle \Delta \hat{x}_0^{(1)2}(z) \rangle$  with and without collision as a function of the scaled propagation distance  $z$  for varying relative velocity  $\delta k_x$ .

Each of these plots demonstrates the relative effect collisions induce on the vacuum fluctuations of Manakov solitons. We show these calculations for  $z > 20$ , which provides at least 5 collision lengths as given by  $z\delta k_x/2$ , in order to insure the validity of the asymptotic collision formulas given in Eqs. (23) and (27). In Fig. 1, it is clear that the term quadratic in  $z$  dominates the overall position noise. The two collision terms of Eq. (26) each introduce positive contributions to the fluctuations, as evidenced by the curves with and without collision. It is not surprising that, as the relative velocity between the two solitons is decreased, the fluctuations increase because of an increase in the interaction length.

The variance of polarization angle fluctuations is shown in Fig. 2. Since  $\langle \Delta \hat{\phi}^{(1)2} \rangle$  is independent of propagation distance, we show the fluctuation effects as a function of relative velocity  $\delta k_x$ . As expected, a decrease in relative velocity results in a subsequent increase in the variance. Furthermore, the variance approaches the no-collision value  $\langle \Delta \hat{\phi}^2 \rangle_0$ , as given in Eq. (22), in the limit of low interaction strength.

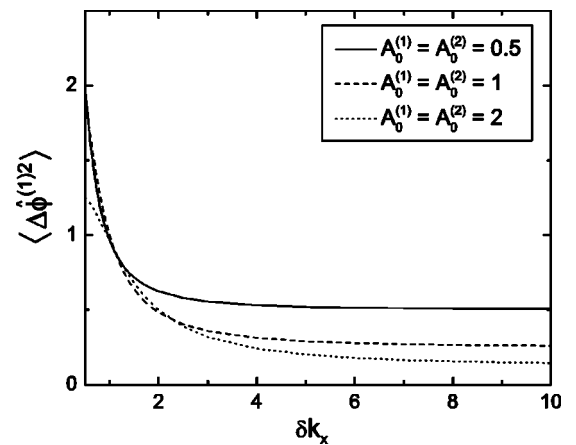


FIG. 2. Variance of polarization angle fluctuations  $\langle \Delta \hat{\phi}^{(1)2} \rangle$  during collision as a function of the relative velocity  $\delta k_x$ . Each curve, corresponding to varying photon numbers, approaches the no-collision limit  $\langle \Delta \hat{\phi}^2 \rangle_0$  given in Eq. (18).

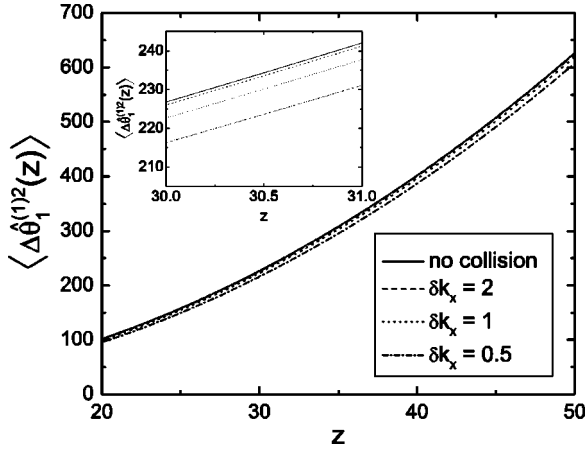


FIG. 3. Variance of phase fluctuations  $\langle \Delta \hat{\theta}_1^{(1)2}(z) \rangle$  with and without collision as a function of the scaled propagation distance  $z$  for varying relative velocity  $\delta k_x$ . Detail of the behavior is shown in the inset.

In Fig. 3, we find, surprisingly, that the soliton collision slightly reduces the variance of the phase fluctuations. In addition, longer interaction lengths, due to a smaller relative velocity, will decrease the variance further, as shown in the inset of Fig. 3. From the third term on the right-hand side of Eq. (28a), we observe that this variance depends on the slope of the classical phase shift during collision with respect to the amplitude of the pulse. This slope is always negative, as can be seen more simply from the classical expression for the collision phase shift for a scalar soliton (Eq. (27b) of [41]). The effect of increasing one soliton amplitude with respect to another causes it to receive less phase shift from the smaller soliton, and vice versa, resulting in an overall reduction of the phase variance.

From Figs. 1–3 it is apparent that the collision-induced fluctuations can seriously affect and perhaps limit the performance of systems that use Manakov solitons. Existing strategies for Manakov soliton computing and logic depend critically on the complex-valued polarization state  $\rho \equiv u_{10}/u_{20} = \cot \phi \exp[i(\theta_1 - \theta_2)]$ , defined as the ratio between the  $u_{10}$  and  $u_{20}$  components [11–14]. Fluctuations in  $\rho$  are calculated through a perturbative approach in which

$$\Delta \hat{\rho}(z) = \frac{\partial \rho}{\partial \phi} \Delta \hat{\phi} + \frac{\partial \rho}{\partial \theta_1} \Delta \hat{\theta}_1(z) + \frac{\partial \rho}{\partial \theta_2} \Delta \hat{\theta}_2(z). \quad (29)$$

Since  $\partial \rho / \partial \theta_1 = -(\partial \rho / \partial \theta_2)$ , it is found that fluctuations of the polarization state are independent of propagation distance. This result suggests that, in the range of validity for the linearized perturbation method [3,35], collision-based soliton computing may be limited only by the relative collision velocity and number of collisions, and not by the total propagation distance. The variance of polarization state fluctuations is plotted versus relative velocity in Fig. 4. With increasing relative velocity, the variance approaches the no-collision variance, given by

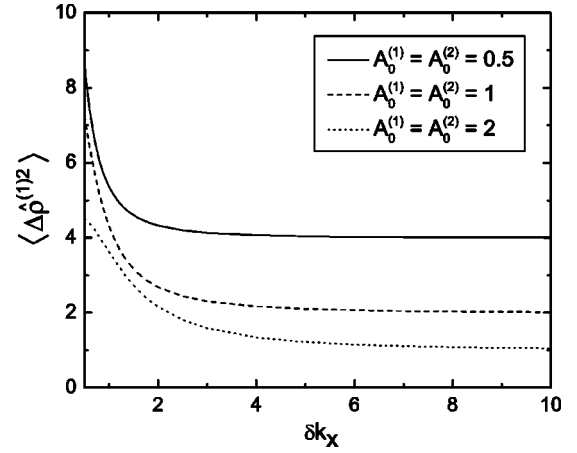


FIG. 4. Variance of polarization state fluctuations  $\langle \Delta \hat{\rho}^{(1)2} \rangle$  during collision as a function of the relative velocity  $\delta k_x$ . Each curve, corresponding to varying photon numbers, approaches the no-collision limit  $\langle \Delta \hat{\rho}^2 \rangle_0$  given in Eq. (30).

$$\langle \Delta \hat{\rho}^2 \rangle_0 = \frac{\csc^4 \phi}{A_0} \left[ \frac{1}{3} \left( 1 + \frac{\pi^2}{12} \right) + \frac{1}{4} \right]. \quad (30)$$

Moreover, the fluctuations increase as the strength of the interaction increases. The extent to which these effects will hinder the performance of any particular system remains a topic for future work.

## V. SOLITON DETECTION AND SQUEEZING

The generation of squeezed states of light has attracted much interest in quantum information and computation, in addition to enabling measurements below the shot noise level. Squeezing of scalar solitons is a well-known effect, experimentally observed for both pairs of conjugate operators [5,6]. Natural questions to ask are how the squeezing of Manakov solitons can be accomplished and how it compares with the scalar case.

The soliton operators can be extracted using a balanced homodyne detection scheme that performs a projection onto the desired operator [4]. The experimental setup is shown in Fig. 5. The orthogonal polarization components of two pulses, an input  $\Delta \hat{\Psi}(x, z)$  and a local oscillator (LO)  $f_L(x, z) \equiv \begin{bmatrix} f_{L1} \\ f_{L2} \end{bmatrix}$ , are separated in a polarization beam splitter (PBS). The PBS for the LO is not shown in Fig. 5. Each of the two components mix in a 50-50 beam splitter and are detected by photodetectors. The difference of the output currents is summed and integrated to complete the measurement, and the output  $\hat{M}(z)$  is [4]

$$\hat{M}(z) = \text{Re} \left( \int f_L^\dagger(x, z) \Delta \hat{\Psi}(x, z) dx \right), \quad (31)$$

subject to the normalization condition

$$\int |f_L(x, z)|^2 dx = 1. \quad (32)$$

Comparison of Eqs. (31) and (16) shows that by appropriate shaping of the LO pulse, any of the six soliton operators can

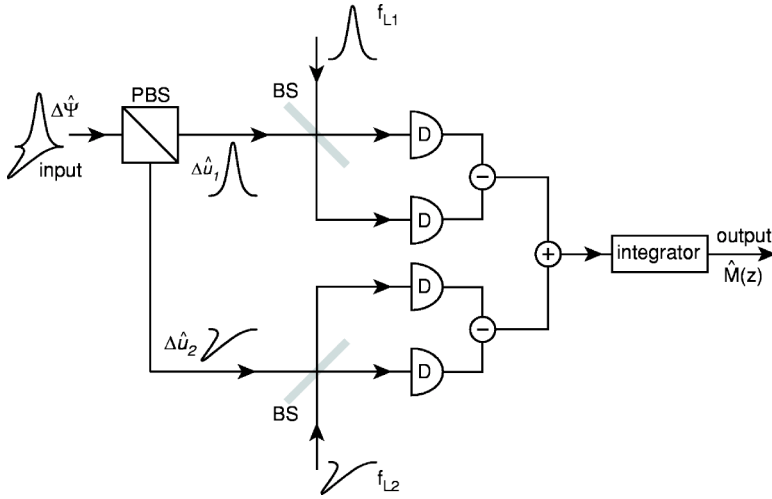


FIG. 5. Schematic of balanced homodyne detection scheme for measurement of soliton operators: PBS, polarization beam splitter; D, photodetector; BS, beam splitter.

be detected. Furthermore, since these six operators evolve in their own subspace, this measurement scheme suppresses any contributions of the continuum. Thus, by setting the LO pulse proportional to  $g_m(x)\exp[i\Phi(z)]$ , we can measure the fluctuation operators  $\Delta\hat{m}(z)$ . Moreover, it was observed that because of the linearity of this detection process, any linear combinations of the operators can be measured as well, provided a LO that is a linear combination of the adjoint functions is used [29].

The soliton operators become correlated with propagation, as can be seen in Eqs. (21), which show the coupling that exists between photon number and phase, and between position and momentum. Using a LO that is a linear combination of particular soliton operators can allow a reduction in the amount of detected noise, and thus make the observation of squeezing possible. To demonstrate optimal squeezing of phase and photon number in a Manakov soliton, we choose the LO to be

$$f_L(x, z) = [c_A g_{A_0}(x) + c_{\theta_1} g_{\theta_1}(x) + c_{\theta_2} g_{\theta_2}(x)] \exp[i\Phi(z)], \quad (33)$$

which will detect, from Eq. (31), the operator

$$\hat{M}(z) = c_A \Delta\hat{A}_0(z) + c_{\theta_1} \Delta\hat{\theta}_1(z) + c_{\theta_2} \Delta\hat{\theta}_2(z). \quad (34)$$

According to Eq. (32), the coefficients  $c_A$ ,  $c_{\theta_1}$ , and  $c_{\theta_2}$  must obey the condition

$$c_A^2 \langle \Delta\hat{A}_0^2 \rangle_0 + c_{\theta_1}^2 \langle \Delta\hat{\theta}_1^2 \rangle_0 + c_{\theta_2}^2 \langle \Delta\hat{\theta}_2^2 \rangle_0 = 1. \quad (35)$$

We consider only the LO of Eq. (33), which gives rise to optimal squeezing, because this measurement will lead to the maximum reduction in the noise floor that exists in optical detection.

The squeezing ratio is defined as

$$R(z) \equiv \frac{\langle \hat{M}^2(z) \rangle}{\langle \hat{M}^2(0) \rangle}. \quad (36)$$

According to this definition, squeezing is observed when measurement of the quantum noise at the output is less than the input. The input (vacuum) state and output state are mea-

sured in an identical fashion. The minimum value of  $R(z)$ , subject to the constraint in Eq. (35), is found using the method of Lagrange multipliers, resulting in

$$R_{\text{opt}}(z) = 1 + 2\Phi_0^2(z) - 2\Phi_0(z)[1 + \Phi_0^2(z)]^{1/2}, \quad (37)$$

where

$$\Phi_0(z) = \frac{1}{A_0} \Phi(z) \left[ \langle \Delta\hat{A}_0^2 \rangle_0 \left( \frac{1}{\langle \Delta\hat{\theta}_1^2 \rangle_0} + \frac{1}{\langle \Delta\hat{\theta}_2^2 \rangle_0} \right) \right]^{1/2}. \quad (38)$$

Using Eqs. (18), we find that

$$\Phi_0(z) = \frac{\Phi(z)}{\left[ \frac{1}{3} \left( 1 + \frac{\pi^2}{12} \right) \right]^{1/2}}, \quad (39)$$

which corresponds exactly to the optimum achieved previously in scalar soliton squeezing [4,45]. This result suggests that, regardless of the amplitudes of each component of the Manakov soliton (or, equivalently, the value of  $\phi$ ), the optimum amount of achievable squeezing when using the LO given in Eq. (33) is identical to the scalar soliton theory. The squeezing ratio  $R_{\text{opt}}(z)$  is plotted as a function of the classical phase shift  $\Phi(z)$  in Fig. 6. Although there is no advantage in the optimal squeezing of Manakov solitons, this calculation is aimed at systems using vector solitons, the performance of which could be improved through proper measurement.

In order to study the squeezing effects for an arbitrary LO, a numerical approach would need to be taken, where one could investigate, for example, the squeezing in each polarization component. This lies outside the scope of the current paper and remains a topic for future work. The use of a nonideal LO adds another level of complexity to the problem because it requires incorporation of the continuum.

## VI. CONCLUSION

In this paper, we have developed an analytical quantum theory of Manakov solitons based on a linearization approximation that separates the soliton into classical and quantum mechanical parts. Using perturbation theory, effects due to the quantum field were investigated in which analytical ex-

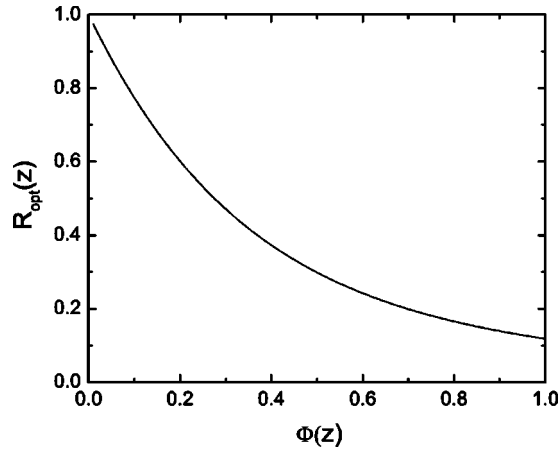


FIG. 6. Optimal squeezing ratio  $R_{\text{opt}}(z)$  vs classical phase shift  $\Phi(z)$  using the measurement scheme of Fig. 5.

pressions were derived, describing the evolution of the six physical soliton parameters with and without the effects of collision. Vacuum-induced fluctuations were also described using this theory. Manakov solitons were shown, like scalar solitons, to undergo phase diffusion and wave packet spreading due to the Kerr nonlinearity and dispersion of the medium, respectively. However, different effects describing the evolution of the polarization angle and polarization state appear in Manakov solitons, and both of these parameters were found to be independent of propagation distance. By varying the relative velocity of the two solitons, collision effects were studied for the position, polarization angle, and polarization state fluctuations. It was found that the variances of these fluctuations increase with decreasing relative velocity, as expected. Calculations of the Manakov soliton phase fluctuations showed the effect that the collision-induced phase variance can actually fall below the level of fluctuations in the absence of collision. We have also shown that, like the fundamental scalar soliton, the fundamental Manakov soliton undergoes a squeezing effect. Surprisingly, the optimal squeezing was proven identical to scalar soliton theory.

These results suggest avenues for future work on applications of Manakov solitons. Since fluctuations of the polarization angle and polarization state are independent of propagation distance, applications exploiting these quantities will not suffer the same limitations as applications based on, for ex-

ample, pulse position, which is subject to increasing jitter as a function of the distance propagated. This theory can both provide an upper-bound limit on the performance of communication or computation systems using Manakov solitons and serve as a guide to designing new experiments to test the fundamental quantum properties of such nonlinear waves.

#### ACKNOWLEDGMENTS

The authors would like to acknowledge useful discussions with J. W. Fleischer, H. Rabitz, and M. Segev. D.R. also acknowledges discussions with V. Anant, V. Baby, F. Meshkati, and S.-H. Son. This work was supported by the Army Research Office MURI grant on optical solitons.

#### APPENDIX

The vectors  $f_m(x, z)$ , defined in Eq. (14), are

$$f_{A_0}(x, z) = \begin{bmatrix} \cos(\phi)\exp(i\theta_1) \\ \sin(\phi)\exp(i\theta_2) \end{bmatrix} \begin{bmatrix} \frac{1}{2} + i\frac{A_0^2}{4}z \\ -\frac{A_0}{4}x \tanh\left(\frac{A_0}{2}x\right) \end{bmatrix} \text{sech}\left(\frac{A_0}{2}x\right),$$

$$f_{x_0}(x, z) = \begin{bmatrix} \cos(\phi)\exp(i\theta_1) \\ \sin(\phi)\exp(i\theta_2) \end{bmatrix} \frac{A_0^2}{4} \tanh\left(\frac{A_0}{2}x\right) \text{sech}\left(\frac{A_0}{2}x\right),$$

$$f_{k_x}(x, z) = \begin{bmatrix} \cos(\phi)\exp(i\theta_1) \\ \sin(\phi)\exp(i\theta_2) \end{bmatrix} \begin{bmatrix} ix \\ +A_0z \tanh\left(\frac{A_0}{2}x\right) \end{bmatrix} \frac{A_0}{2} \text{sech}\left(\frac{A_0}{2}x\right),$$

$$f_{\phi}(x, z) = \begin{bmatrix} -\sin(\phi)\exp(i\theta_1) \\ \cos(\phi)\exp(i\theta_2) \end{bmatrix} \frac{A_0}{2} \text{sech}\left(\frac{A_0}{2}x\right),$$

$$f_{\theta_1}(x, z) = \begin{bmatrix} \cos(\phi)\exp(i\theta_1) \\ 0 \end{bmatrix} i\frac{A_0}{2} \text{sech}\left(\frac{A_0}{2}x\right),$$

$$f_{\theta_2}(x, z) = \begin{bmatrix} 0 \\ \sin(\phi)\exp(i\theta_2) \end{bmatrix} i\frac{A_0}{2} \text{sech}\left(\frac{A_0}{2}x\right). \quad (\text{A1})$$

The vectors  $g_m(x)$ , defined in Eq. (15), are

$$g_{A_0}(x) \equiv \begin{bmatrix} g_{1A} \\ g_{2A} \end{bmatrix} = \begin{bmatrix} \cos(\phi)\exp(i\theta_1) \\ \sin(\phi)\exp(i\theta_2) \end{bmatrix} A_0 \text{sech}\left(\frac{A_0}{2}x\right),$$

$$g_{x_0}(x) \equiv \begin{bmatrix} g_{1x} \\ g_{2x} \end{bmatrix} = \begin{bmatrix} \cos(\phi)\exp(i\theta_1) \\ \sin(\phi)\exp(i\theta_2) \end{bmatrix} x \text{sech}\left(\frac{A_0}{2}x\right),$$

$$g_{k_x}(x) \equiv \begin{bmatrix} g_{1k} \\ g_{2k} \end{bmatrix} = \begin{bmatrix} \cos(\phi)\exp(i\theta_1) \\ \sin(\phi)\exp(i\theta_2) \end{bmatrix} i\frac{A_0}{2} \tanh\left(\frac{A_0}{2}x\right) \text{sech}\left(\frac{A_0}{2}x\right),$$

$$\begin{aligned}
 g_\phi(x) &\equiv \begin{bmatrix} g_{1\phi} \\ g_{2\phi} \end{bmatrix} = \begin{bmatrix} -\sin(\phi)\exp(i\theta_1) \\ \cos(\phi)\exp(i\theta_2) \end{bmatrix} \frac{1}{2} \operatorname{sech}\left(\frac{A_0}{2}x\right), \\
 g_{\theta_1}(x) &\equiv \begin{bmatrix} g_{1\theta} \\ 0 \end{bmatrix} = \begin{bmatrix} \frac{1}{\cos(\phi)} \exp(i\theta_1) \\ 0 \end{bmatrix} \left[ 1 - \frac{A_0}{2}x \tanh\left(\frac{A_0}{2}x\right) \right] i \operatorname{sech}\left(\frac{A_0}{2}x\right), \\
 g_{\theta_2}(x) &\equiv \begin{bmatrix} 0 \\ g_{2\theta} \end{bmatrix} = \begin{bmatrix} 0 \\ \frac{1}{\sin(\phi)} \exp(i\theta_2) \end{bmatrix} \left[ 1 - \frac{A_0}{2}x \tanh\left(\frac{A_0}{2}x\right) \right] i \operatorname{sech}\left(\frac{A_0}{2}x\right).
 \end{aligned} \tag{A2}$$

---

[1] S. J. Carter, P. D. Drummond, M. D. Reid, and R. M. Shelby, *Phys. Rev. Lett.* **58**, 1841 (1987).

[2] P. D. Drummond and S. J. Carter, *J. Opt. Soc. Am. B* **4**, 1565 (1987).

[3] Y. Lai and H. A. Haus, *Phys. Rev. A* **40**, 844 (1989).

[4] H. A. Haus and Y. Lai, *J. Opt. Soc. Am. B* **7**, 386 (1990).

[5] M. Rosenbluh and R. M. Shelby, *Phys. Rev. Lett.* **66**, 153 (1991).

[6] S. R. Friberg, S. Machida, M. J. Werner, A. Levanon, and T. Mukai, *Phys. Rev. Lett.* **77**, 3775 (1996).

[7] P. D. Drummond, R. M. Shelby, S. R. Friberg, and Y. Yamamoto, *Nature (London)* **365**, 307 (1993).

[8] A. Sizmann and G. Leuchs, *Progress in Optics* (North-Holland, Amsterdam, 1999), Vol. XXXIX, pp. 373–469.

[9] S. V. Manakov, *Zh. Eksp. Teor. Fiz.* **65**, 505 (1973) [*Sov. Phys. JETP* **38**, 248 (1974)].

[10] R. Radhakrishnan, M. Lakshmanan, and J. Hietarinta, *Phys. Rev. E* **56**, 2213 (1997).

[11] M. H. Jakubowski, K. Steiglitz, and R. Squier, *Phys. Rev. E* **58**, 6752 (1998).

[12] K. Steiglitz, *Phys. Rev. E* **63**, 016608 (2000).

[13] K. Steiglitz, *Phys. Rev. E* **63**, 046607 (2001).

[14] D. Rand, K. Steiglitz, and P. R. Prucnal, *Int. J. Unconv. Comp.* **1**, 31 (2005).

[15] C. Anastassiou, M. Segev, K. Steiglitz, J. A. Giordmaine, M. Mitchell, M. F. Shih, S. Lan, and J. Martin, *Phys. Rev. Lett.* **83**, 2332 (1999).

[16] C. Anastassiou, J. W. Fleischer, T. Carmon, M. Segev, and K. Steiglitz, *Opt. Lett.* **26**, 1498 (2001).

[17] M. Shih and M. Segev, *Opt. Lett.* **21**, 1538 (1996).

[18] D. N. Christodoulides, S. R. Singh, M. I. Carvalho, and M. Segev, *Appl. Phys. Lett.* **68**, 1763 (1996).

[19] Z. Chen, M. Segev, T. Coskun, and D. N. Christodoulides, *Opt. Lett.* **21**, 1436 (1996).

[20] J. U. Kang, G. I. Stegeman, J. S. Aitchison, and N. Akhmediev, *Phys. Rev. Lett.* **76**, 3699 (1996).

[21] V. V. Steblina, A. V. Buryak, R. A. Sammut, D. Y. Zhou, M. Segev, and P. Prucnal, *J. Opt. Soc. Am. B* **17**, 2026 (2000).

[22] C. R. Menyuk, *IEEE J. Quantum Electron.* **25**, 2674 (1989).

[23] E. P. Bashkin and A. V. Vagov, *Phys. Rev. B* **56**, 6207 (1997).

[24] T. A. B. Kennedy and E. M. Wright, *Phys. Rev. A* **38**, 212 (1988).

[25] T. A. B. Kennedy and S. Wabnitz, *Phys. Rev. A* **38**, 563 (1988).

[26] Y. Lai and H. A. Haus, *Phys. Rev. A* **40**, 854 (1989).

[27] P. D. Drummond and A. D. Hardman, *Europhys. Lett.* **21**, 279 (1993).

[28] C.-P. Yeang, *J. Opt. Soc. Am. B* **16**, 1269 (1999).

[29] Y. Lai and H. A. Haus, *Phys. Rev. A* **42**, 2925 (1990).

[30] H. A. Haus, K. Watanabe, and Y. Yamamoto, *J. Opt. Soc. Am. B* **6**, 1138 (1989).

[31] R. Tanaś and S. Kielich, *J. Mod. Opt.* **37**, 1935 (1990).

[32] A. B. Matsko and V. V. Kozlov, *Phys. Rev. A* **62**, 033811 (2000).

[33] B. Yoon and J. W. Negele, *Phys. Rev. A* **16**, 1451 (1977).

[34] J. Scheuer and M. Orenstein, *J. Opt. Soc. Am. B* **18**, 954 (2001).

[35] F. X. Kärtner and L. Boivin, *Phys. Rev. A* **53**, 454 (1996).

[36] D. J. Kaup, *J. Math. Anal. Appl.* **54**, 849 (1976).

[37] T. I. Lakoba and D. J. Kaup, *Phys. Rev. E* **56**, 6147 (1997).

[38] A. B. Matsko, V. V. Kozlov, and M. O. Scully, *Phys. Rev. Lett.* **82**, 3244 (1999).

[39] V. V. Kozlov and A. B. Matsko, *J. Opt. Soc. Am. B* **16**, 519 (1999).

[40] P. D. Drummond and W. Man, *Opt. Commun.* **105**, 99 (1994).

[41] V. E. Zakharov and A. B. Shabat, *Zh. Eksp. Teor. Fiz.* **61**, 118 (1971) [*Sov. Phys. JETP* **34**, 62 (1972)].

[42] P. D. Drummond, J. Breslin, and R. M. Shelby, *Phys. Rev. Lett.* **73**, 2837 (1994).

[43] V. V. Kozlov and D. A. Ivanov, *Phys. Rev. A* **65**, 023812 (2002).

[44] T. Kanna and M. Lakshmanan, *Phys. Rev. E* **67**, 046617 (2003).

[45] Y. Lai, *J. Opt. Soc. Am. B* **10**, 475 (1993).